LOCAL ANALYSIS OF CONFINEMENT AND TRANSPORT IN NEUTRAL BEAM HEATED DIII–D DISCHARGES WITH NEGATIVE MAGNETIC SHEAR*

D.P. SCHISSEL, C.M. GREENFIELD, J.C. DEBOO, L.L. LAO, E.A. LAZARUS,[1] G.A. NAVRATIL,[2] B.W. RICE,[3] G.M. STAEBLER, B.W. STALLARD,[3] E.J. STRAIT, H.E. ST. JOHN, M.E. AUSTIN,[4] K.H. BURRELL, T.A. CASPER,[3] D.R. BAKER, V.S. CHAN, E.J. DOYLE,[5] J.R. FERRON, C.B. FOREST, P. GOHIL, R.J. GROEBNER, W.W. HEIDBRINK,[6] R.–M. HONG, A.W. HOWALD, C.–L. HSIEH, A.W. HYATT, G.L. JACKSON, J. KIM, C.J. LASNIER,[3] A.W. LEONARD, J. LOHR, R.J. LA HAYE, R. MAINGI,[7] R.L. MILLER, M. MURAKAMI,[1] T.H. OSBORNE, C.C. PETTY, C.L. RETTIG,[5] T.L. RHODES,[5] S. SABBAGH,[2] T.C. SCOVILLE, R.T. SNIDER, R.D. STAMBAUGH, R.E. STOCKDALE, P.L. TAYLOR, T.S. TAYLOR, D.M. THOMAS, M.R. WADE,[1] R.E. WALTZ, R.D. WOOD,[3] D.G. WHYTE[8]

General Atomics
P.O. Box 85608
San Diego, California 92186-9784
United States of America

[1]Oak Ridge National Laboratory, Oak Ridge, Tennessee, USA.
[2]Columbia Universtiy, New York, New York, USA.
[3]Lawrence Livermore National laboratory, Livermore, California, USA.
[4]University of Maryland, College Park, Maryland, USA.
[5]University of California, Los Angeles, California, USA.
[6]University of California, Irvine, California, USA.
[7]Oak Ridge Associated Universities, Oak Ridge, Tennessee, USA.
[8]INRS – Energie et Materiaux, Varennes, Quebec

*Work supported by the U.S. Department of Energy under Contract No. DE-AC03-89ER51114, DE-AC05-96OR22464, DE-AC04-94AL85000, and Grant Nos. DE-FG03-86ER53266 and DE-FG03-95ER54294.

F1-CN-64/A5-3

LOCAL ANALYSIS OF CONFINEMENT AND TRANSPORT IN NEUTRAL BEAM HEATED DIII–D DISCHARGES WITH NEGATIVE MAGNETIC SHEAR

ABSTRACT

High triangularity double–null discharges with weak or negative central magnetic shear and with both an L–mode and an H–mode edge have been produced on DIII–D. The L–mode edge cases are characterized by peaked toroidal rotation, ion temperature, and plasma density profiles with reduced ion transport in the negative shear region. The H–mode edge cases have broader profiles consistent with reduced ion transport, to the neoclassical level, over the entire plasma cross section. The L–mode edge cases have a greater reduction in central ion diffusivity with stronger negative shear while the H–mode edge cases do not exhibit this dependence. Plasma fluctuation measurements show a dramatic reduction in turbulence accompanies the improved ion confinement. Calculations of sheared $\mathbf{E}\times\mathbf{B}$ flow indicate that this mechanism can overcome the η_i mode growth rate in the region of reduced transport.

1. INTRODUCTION

An attractive, compact, economical fusion power plant requires the development of a plasma with both good energy confinement and MHD stability at high beta. Since the last IAEA meeting, a class of experiments with improved confinement and stability have been operated on the DIII–D tokamak by carefully tailoring the shape of the plasma current profile [1–3]. The shaping of the current profile in these discharges is such that a central region of weak or negative magnetic shear (NCS) [$s = (r/q)\, dq/dr \leq 0$] has been created. The inverted safety factor (q) profile of the NCS configuration is a robust regime that has reliably been obtained with both neutral beam heating and fast wave current drive. This paper reports on the confinement and transport properties of beam heated NCS discharges. NCS discharges with fast wave heating will be presented at this conference in paper F1–CN–64/E–1. The high beta NCS operation results from the majority of the plasma volume being in the second stable regime for ideal MHD ballooning modes. Details of the MHD behavior of these plasmas will be presented in papers F1–CN–64/A1–2 and DP–1 at this conference.

2. NCS DISCHARGE EVOLUTION

NCS discharges are produced in DIII–D using codirectional neutral beam injection early in the initial current ramp [4]. This early beam injection typically started around 300–500 ms after plasma breakdown and with moderate 75 keV beam power (2–5 MW). Figure 1 shows the temporal evolution of a double–null NCS plasma with both an L–mode and H–mode phase. We will use the terminology NCS plasma with H–mode (L–mode) edge to indicate a plasma with weak or negative central magnetic shear combined with edge conditions characteristic of an ELM–free H–mode (L–mode). The toroidal field is 2.1 T and the gas and beam fuel is deuterium. The low beam target density (n_e = 1–2 × 10^{19} m^{-3}) combined with the early neutral beam

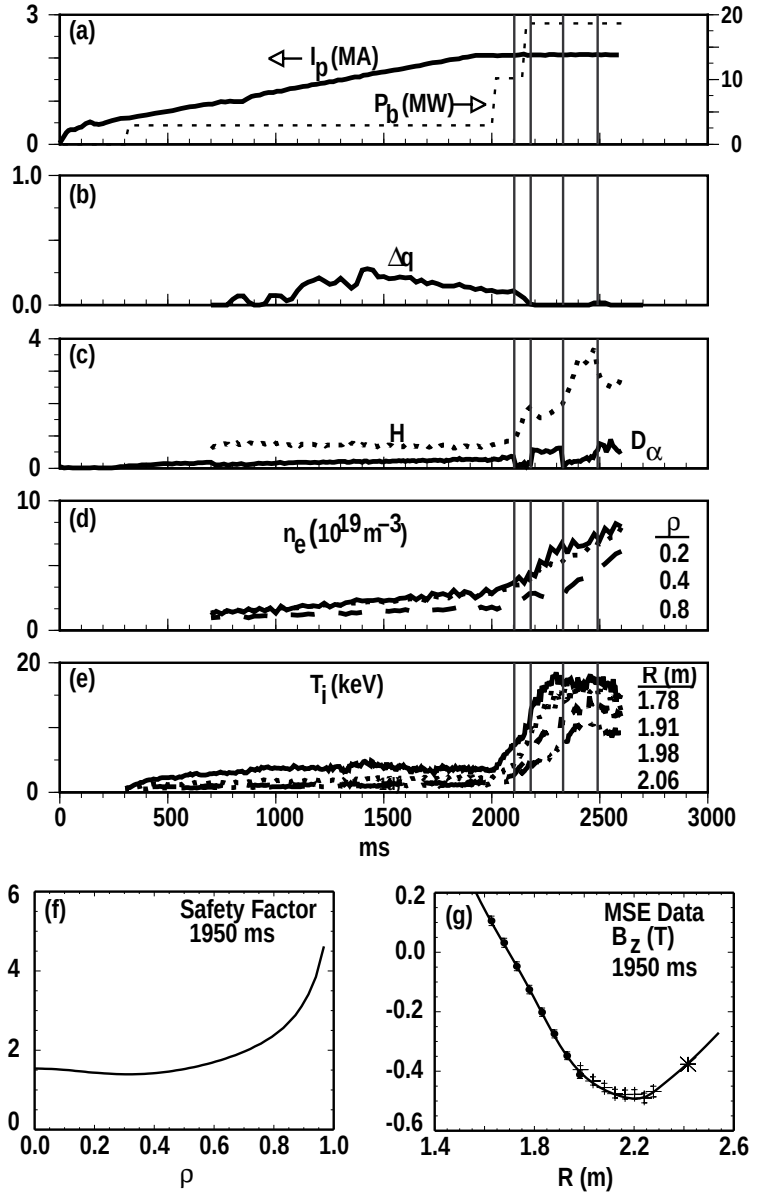

Fig. 1. (a) Early beam power during the current ramp produces the NCS configuration. (b) This double-null plasma (87935) has weak shear [$\Delta q = q(0) - q_{min}$]. (c) There are two H–mode edge phases (divertor D_α emission) in this discharge marked by the vertical lines. Enhancement (H) over ITER–89P exceeds 3. (d) Density profiles are peaked in L–mode edge and broad in H–mode edge. (e) Ion temperature is more peaked in L–mode edge. (f,g) The MSE diagnostic measures the local magnetic field pitch angle and, combined with magnetic probe measurements, results in a well determined q profile.

power yields central electron temperatures (T_e) around 3 keV early in the plasma current rise phase. Electron temperatures in this range create a central current diffusion time on the order of 5 s. The central current density is effectively frozen at this early low value, forcing a hollow current profile to develop as the plasma current ramps up.

The hollow current profile results in negative shear since the q profile also has a minimum off axis [Fig. 1(b) plotted as $\Delta q = q(0) - q_{min}$]. In these experiments the q profile is directly determined from the profile of local field pitch angle measured by the 16 channel motional Stark effect (MSE) diagnostic [Fig. 1(f,g)], combined with information on the plasma shape as determined by EFIT from external magnetic measurements. By varying the early beam timing, the level of beam power, and the beam target density, some shot-to-shot control over the current profile shape has been possible.

The second phase of the NCS discharge begins with the initiation of high power neutral beam heating typically just after the plasma current has reached flattop; incrementally increased at 2.0 s and 2.15 s in Fig. 1(a). Weak shear is maintained during the high power phase [Fig. 1(b)] and varies slowly in time. It is during this high power phase that this NCS discharge exhibits good confinement with the formation of an internal transport barrier. There is an increase in the core ion temperature (T_i) [Fig. 1(e)] relative to the middle part of the discharge indicating the formation of the transport barrier; a central value of approximately 17 keV is obtained. At this time the global confinement begins to improve until ultimately an H factor (against ITER89–P) of above 3.0 is obtained. The formation of a transport barrier can also be inferred directly from the increased ∇T_i when compared to discharges without NCS. Figure 2 compares both an H–mode and L–mode edge NCS plasma to an H–mode discharge with a monotonic q profile. The transport barrier formation near $\rho = 0.5$ is clearly evident by the increase in both T_i and toroidal rotation (Ω_φ) at that spatial location. NCS discharges with lower power during the second phase still have reversed shear but do not exhibit an increase in confinement. These low power NCS discharges have approximately the same confinement as an ordinary L–mode discharge with a monotonic q profile. This indicates that there is a power threshold for improved confinement in NCS discharges.

Transport has been studied in high triangularity ($\delta \approx 0.8$) double-null plasmas with plasma currents up to the 2.1 MA level. The ability to control the L– and H–mode transition in these plasmas has been made possible by the flexibility of the DIII–D digital plasma control system. The early level of beam heating in NCS discharges exceeds the H–mode power threshold for double–null diverted plasmas in DIII–D. For NCS plasmas to remain with an L–mode edge the plasma has been displaced toward the upper null which is opposite to the ion ∇B direction. At 2.1 s, the discharge in Fig. 1 is moved downward, balancing the two nulls, resulting in the H–mode transition 5 ms later. Interestingly, there is a transition back to L–mode 75 ms later even though the power has been increased to the 18 MW level. The speculation is that this return to L–mode results from the reduction in power flow near the edge due to the dramatic reduction in core energy transport inside the region of weak shear. Finally, at 2.33 s the discharge returns to an ELM–free H–mode until the first ELM occurs at 2.49 s.

3. TRANSPORT IN NCS DOUBLE–NULL DISCHARGES

L–mode edge NCS plasmas are characterized by a peaking of the density profile. This is evident from Fig. 1(d) where after the H to L transition at 2.18 s there is a larger increase in n_e at $\rho = 0.2$ than $\rho = 0.4$ with a decrease in density at $\rho = 0.8$. In general, the peaked density profile combined with the large core temperature gradients produce highly peaked pressure (p) profiles. The discharge in Fig. 1 reaches a value of $p(0)/\langle p \rangle = 4$ at 2.35 s but values up to 5 have been observed. The core of these discharges are in the second stable regime for ballooning modes due to the weak or negative magnetic shear. However, L–mode edge NCS discharges typically disrupt when

normalized beta $\beta_N \equiv \beta$ (%)/[I_p/aB_T (MA/mT)] exceeds 2.0–2.5. This disruption is believed to result from the plasma becoming unstable to a global resistive mode. The density peaking is direct evidence that a reduction in particle transport accompanies the reduction in energy transport in L–mode edge NCS plasmas. Typically, the rise rate in core density is approximately equal to the beam fueling rate with the inferred particle diffusivity dropping to near zero.

Density profile peaking in NCS H–mode edge plasmas has not been observed. Although the density continues to increase in Fig. 1 after the L to H transition at 2.33 s, the density profile begins to broaden. In general for H–mode edge NCS plasmas, the broad density profile results in a relatively broad pressure profile. This broader pressure profile leads to a broadening of the beam deposition profile which reduces the heating and fueling of the core plasma. The larger β_N value than the L–mode edge case is consistent with ideal MHD calculations with a broader pressure profile. Termination of the high performance phase in H–mode edge plasmas typically results from the onset of an edge kink mode.

The ability to time the L to H transition has lead to the capability to combine the good confinement properties of the NCS L–mode core with the good confinement properties of the H-mode edge leading to NCS discharges with reduced ion transport over the entire plasma cross section [5]. It is this type of discharge that has resulted in record DIII–D performance. The L–mode phase allows for increased performance in the weak or negative shear region. The H–mode transition timed just prior to the L–mode phase disruption allows the discharge to continue by broadening the pressure profile before a stability limit is reached. Figure 2 illustrates the change in profile shape between an NCS L–mode edge and H–mode edge plasma. Ion temperature and rotation profiles rise linearly from the edge in the H–mode case in agreement with a global reduction in ion transport. Discharges with an early H–mode transition have lower performance than discharges with a later transition because the density rise at the edge reduces beam penetration and makes it difficult to obtain the enhanced central performance in the L–mode phase.

The detailed local study of the temporal evolution of NCS plasmas is made possible by the extensive array of DIII–D profile diagnostics [6] which measure T_i, Ω_φ, n_e, T_e, Z_{eff}, and radiated power. Local power balance energy transport analysis presented in this paper uses the computer codes ONETWO and TRANSP. Inputs into these codes include the temporal evolution of the kinetic plasma profiles and the detailed magnetic equilibrium reconstructions. The diffusivities (χ) are calculated from $q_{e,i} = n_{e,i}\,\chi_{e,i}\,\partial T_{e,i}/\partial r$ where $q_{e,i}$ is the radial energy flux due to conduction for each species and $r = (\Phi/B_{T_o}\,\pi)^{1/2}$ where Φ is the toroidal flux. Uncertainties in χ are estimated by applying several different types of temporal smoothing to both transport input and output quantities. Classical electron–ion energy exchange is assumed and only diagonal transport coefficients are considered. The normalized radius ρ, used below and in the figures, is defined as r normalized to its maximum value.

Previous work [2,3] has demonstrated that both χ_i and χ_e are reduced after the formation of the internal transport barrier. Inside the region of negative shear χ_i drops by a factor of 10 after the transition to below Chang–Hinton neoclassical values while χ_e is reduced by approximately 50%. In general for all enhanced NCS plasmas, the overall power flow has the majority of beam power absorbed by the ion channel, the ions increasing their temperature and transferring power to the electrons via classical energy exchange and the power exiting the plasma via electron conduction.

A comparison between the L–mode and H–mode edge phases of the Fig. 1 NCS plasma is shown in Fig. 3. Inside the weak shear region ($\rho < 0.5$), both the L–mode

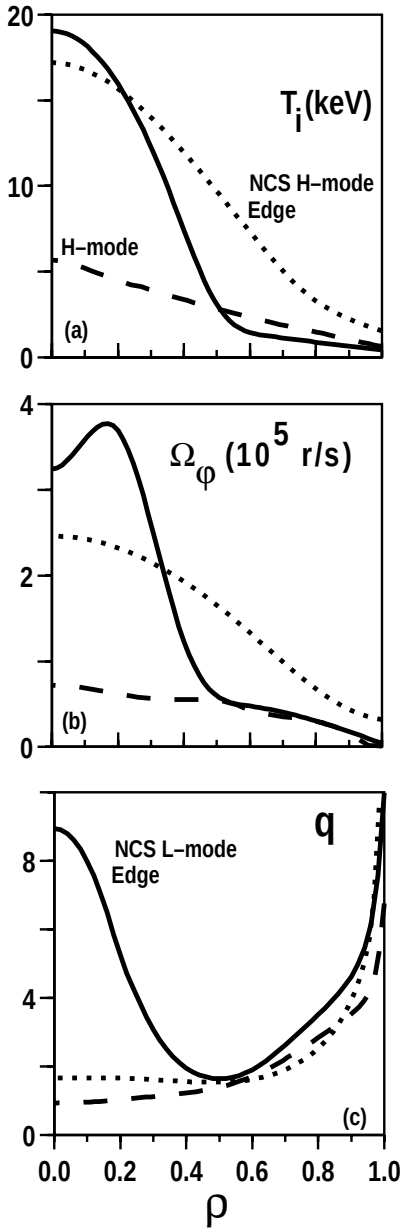

Fig. 2. (a,b) Ion temperature and rotation profiles for an H–mode with a monotonic q profile (82205) and two NCS discharges with an L– (83721) and H–mode (87977) edge. The NCS L–mode edge case has a clear transport barrier at ρ = 0.5 while the NCS H–mode edge plasma shows improved transport at all radii. (c) A variety of q profiles can be created in DIII–D.

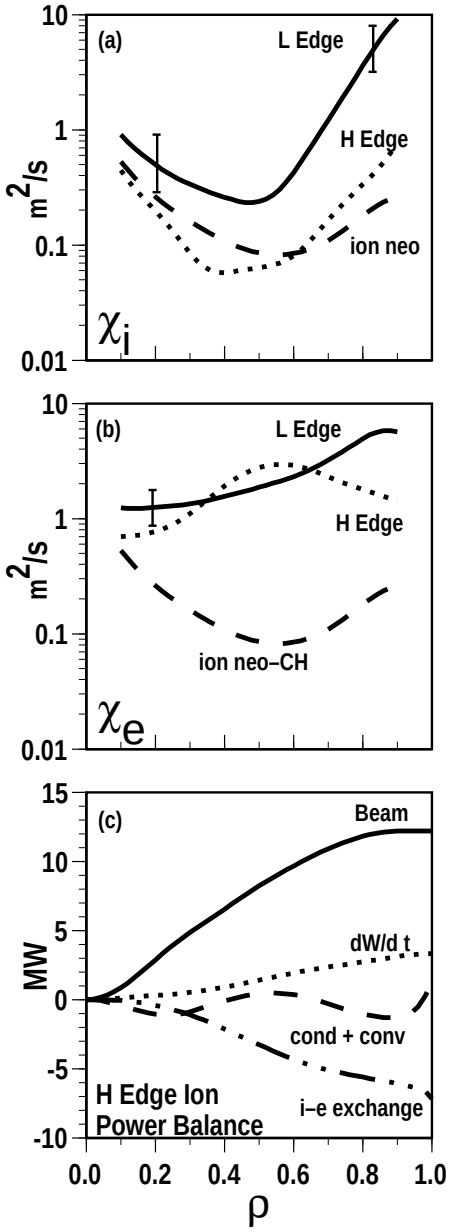

Fig. 3. (a, b) Ion and electron diffusivity for the NCS discharge (87935) of Fig. 1. The L–mode edge time is taken at 2.3 s and the H–mode edge time 2.45 s. NCS H–mode edge χ_i is near neoclassical over the entire cross section. (c) NCS H–mode edge ion power balance shows both conduction and convection are reduced to a negligible level.

and H–mode edge cases have low values of χ_i; the H–mode is near the neoclassical level [Fig. 3(a)]. Outside the weak shear region, the H–mode case continues to remain near the neoclassical level and is approximately a factor of 10 lower than the L–mode ion diffusivity. For both cases χ_e remains relatively unchanged [Fig. 3(b)], except at the plasma edge ($\rho > 0.8$), where there is a decrease of approximately a factor of 3–4 in the H–mode phase. In the H–mode phase the total conducted and convected ion power is reduced to negligible levels, so that in the ion channel the neutral beam power is balanced by the ion–electron exchange and the increase in stored energy [Fig. 3(c)].

In comparing pre–transport barrier formation to post–formation in NCS plasmas, there is both a temporal [7] and spatial [2] correlation between the reduction in transport and the reduction in electrostatic fluctuations as determined by far–infrared (FIR) scattering and beam emission spectroscopy. The spatial correlation can be illustrated with FIR measurements that compare NCS discharges with both an L–mode and H–mode edge. Recalling that the FIR diagnostic measures the frequency spectrum and relative magnitude of poloidally propagating density fluctuations, Fig. 4 compares the scattered power spectrum $\left(\propto \tilde{n}_e^2\right)$ for the L–mode and H–mode phases of the Fig. 3 plasma. The NCS L–mode edge case has low interior broadband turbulence that is comparable to the H–mode phase consistent with χ_i being reduced in the core. The spikes in the H–mode case represent low–n coherent MHD modes. The H–mode phase data demonstrates a reduction of the edge fluctuations resulting in low turbulence over the entire plasma cross section which is consistent with the global reduction in ion diffusivity.

4. THE DEPENDENCE OF TRANSPORT ON SHEAR

Energy transport has been compared in two similar double–null NCS L–mode edge plasmas but with different core shear profiles [8]. The discharges differed by a

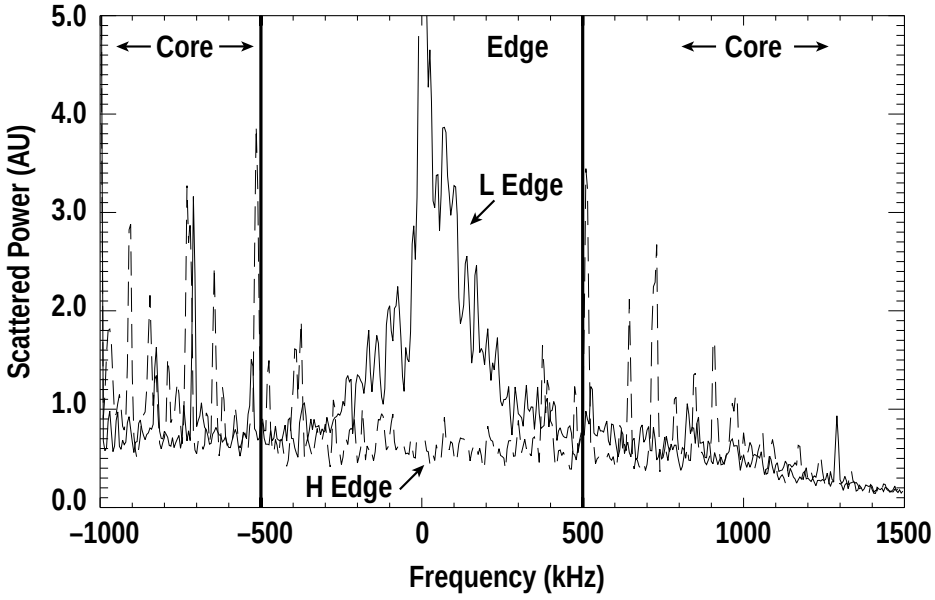

Fig. 4. Comparison of measured plasma fluctuations (k_θ = 2 cm^{-1}) for the L– and H–mode edge times in Fig. 3. The fluctuations in the NCS H–mode edge case are reduced over the entire cross section.

0.2 second delay in both the low and high power beam heating phases. The delayed beam timing results in a smaller Δq [Fig. 5(a)] of 0.56 versus 1.56 and a 20% higher electron density. Power balance analysis during the early formation of the transport barrier and after the full formation for the small Δq case shows the typical reduction in χ_i [Fig. 5(b)] inside the region of weak or negative shear. Note that the neutral beam power level during the early formation is at 5 MW compared to 10 MW after full formation. During the enhanced confinement phase, larger Δq results in a reduction in χ_i of about a factor of 5 inside the negative shear region; within experimental uncertainty χ_e remains unchanged. Temporally, the discharge with lower shear has approximately an 80 ms delay in the onset of reduced ion transport when compared to the discharge with higher shear. Although the larger Δq discharge has a larger improvement in central confinement, these discharges typically reach peak values sooner and at lower values of β_N and reactivity.

The FIR measured electrostatic fluctuations for these two discharges are similar with a behavior like that of the L–mode case in Fig. 4. These turbulence reductions in NCS discharges are, for example, consistent with the suppression of toroidal ion temperature gradient (ITG or η_i) driven transport. Data from the CER diagnostic also provides information on the **E**×**B** shear profile in DIII–D. It is generally observed that the reduction in electrostatic fluctuations and the reduction in diffusive transport occur in regions where the **E**×**B** flow shear $\partial/\partial\psi\,(E_r/RB_\theta)$ is the greatest. This large flow shear results from the strong peaking of toroidal rotation inside the region with weak or negative magnetic shear. The effects of the flow shear can be quantified [9] by comparing the change in flow shear, as determined by the Doppler shift shear rate

$$\omega_{ExB} = \frac{\left(RB_\theta\right)^2}{B}\frac{\partial}{\partial\psi}\left(\frac{E_r}{RB_\theta}\right) \quad ,$$

to simulated turbulence growth rates (γ_{max}). When ω_{ExB} is greater than γ_{max}, **E**×**B** flow shear stabilization of turbulence is expected [10] resulting in the formation of a transport barrier [11].

The NCS configuration allows access to large ∇p since these plasmas are calculated to be MHD unstable with a forced positive magnetic shear profile. However, the NCS configuration alone is not sufficient for improved confinement. The existence of a power threshold for improved NCS confinement is consistent with the observation that to reduce turbulent fluctuations, a sufficient shear flow rate is required. We conclude from measurements and calculations that the stabilization of mircoturbulence by **E**×**B** flow shear is the prime candidate to explain the reduced transport.

The turbulence growth rates have been approximated by a linear growth rate calculated from a 3–D ballooning mode gyrokinetic stability (GKS) code in the electrostatic limit [12]. The maximum growth rate (γ_{max}) is calculated considering both the ITG and dissipative trapped electron modes. A comparison between γ_{max} and ω_{ExB} in the low magnetic shear L–mode discharge [Fig. 5, Case 2] during the low power beam phase is shown in Fig. 5(c); γ_{max} is equal to or exceeds ω_{ExB} for $\rho >$ 0.25. During the high power phase [Fig. 5(d)], $\omega_{ExB} > \gamma_{max}$ inside the region of reduced ion transport ($\rho < 0.5$) consistent with turbulence suppression by **E**×**B** flow shear. The region of linear stability ($\gamma_{max} = 0$) for $\rho < 0.25$ in Fig. 5(c) results from a combination of negative shear and Shafranov shift and even more strongly from thermal ion dilution by fast ions and $T_i > T_e$. Changing the magnetic shear at zero Shafranov shift can at most move the linear stability boundary to $\rho = 0.15$ whereas

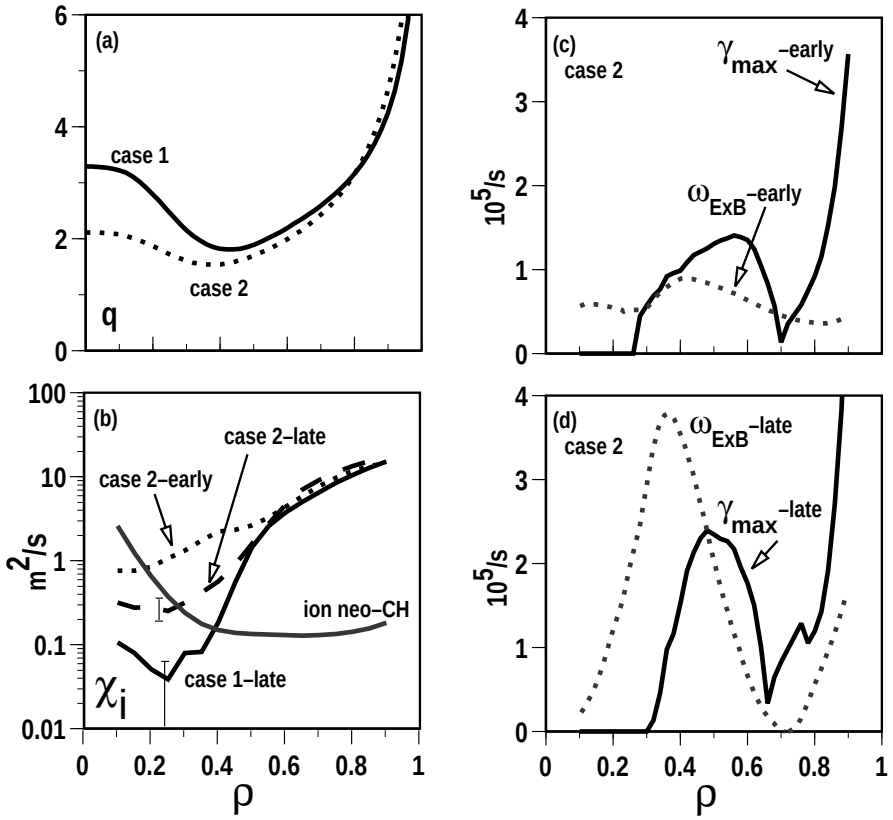

Fig. 5. (a) L–mode edge NCS plasmas with larger negative magnetic shear (Case 1 –87003) and weak shear (Case 2 – 87031). (b) χ_i is reduced from before (early at 5 MW) the transport barrier to after (late at 10 MW) the transport barrier formation. For fixed conditions χ_i is reduced for larger magnetic shear. (c) During the early formation of the transport barrier the turbulence growth rate (γ_{max}) exceeds the Doppler shift shear rate (ω_{ExB}). (d) After the transport barrier formation $\gamma_{max} < \omega_{ExB}$ in the region of reduced ion transport.

setting $n_i = n_e$ and $T_i = T_e$ with the experimental magnetic shear extends the instability to the magnetic axis with γ_{max} exceeding ω_{ExB}. This suggests that the effects of low target density and neutral beam heating (i.e. thermal ion dilution and $T_i > T_e$) lower γ_{max} and thus lower the threshold ω_{ExB} for transport barrier formation.

Although our results indicate that **E**×**B** flow shear is a leading candidate to explain stabilization of mircoturbulence from non–NCS to NCS discharges, the further reduction in χ_i with larger shear can not be explained by the same mechanism. Qualitatively, Fig. 5(d) represents both the low and high shear discharges after the barrier formation. With no difference in the **E**×**B** shearing rates it is hard to understand how **E**×**B** flow shear can be playing a role in the further χ_i reduction. In addition to the unknown mechanism effecting ion transport with lower magnetic shear, for both cases at $\rho = 0.2$, calculations indicate that in the range $0.01 < k_\theta \rho_s < 100.0$ no linearly unstable electrostatic modes are present. Since χ_e does not change much upon entering the enhanced NCS regime, and certainly does not drop to electron neoclassical, there must be some instability effecting electron transport.

Energy transport has also been compared in two similar NCS H–mode edge plasmas [13] with different core shear profiles (Fig. 6). These different q profiles were created by different levels of early beam power; 3.5 MW for the lower Δq case

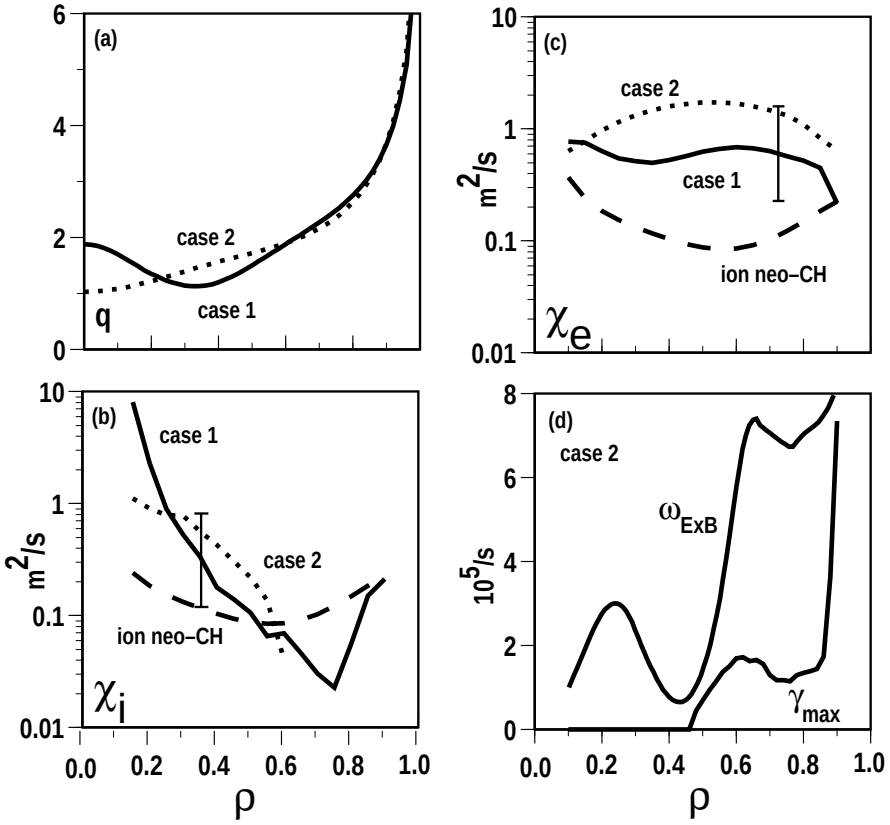

Fig. 6. (a) H–mode edge NCS plasmas with larger negative magnetic shear (Case 1 – 87953) and weak shear (Case 2 – 87937). (b, c) Ion and electron diffusivity does not change with magnetic shear. (d) The Doppler shift shear rate (ω_{ExB}) is greater than the turbulence growth rate (γ_{max}) at all radii for the NCS H–mode edge plasma.

compared to 5.5 MW for the larger Δq value. Prior to the termination of the high performance phases, both discharges have nearly identical evolution. FIR scattering measurements show no difference in density fluctuations between the two plasmas. As was demonstrated in Fig. 3(c), with the H–mode edge the plasma core basically behaves like an integrator of the applied heating power leaving no power to be diffusively conducted or convected away from the core. Based on transport analysis these two discharges have basically the same behavior [Fig. 6(b,c)]; negative values of χ are encountered at different times in the analysis but the calculated uncertainty includes positive values. A comparison of γ_{max} and ω_{ExB} in the enhanced confinement phase [Fig. 6(d)] shows $\omega_{ExB} > \gamma_{max}$ everywhere which is consistent with the neoclassical ion transport over the entire cross section as predicted by earlier simulations [14]. As in the L–mode edge case, the larger Δq discharge reaches its peak performance sooner but at a lower absolute value compared to the smaller Δq discharge. However, in contrast to the L–mode edge case, the H–mode edge cases show no further reduction of transport for the negative magnetic shear case compared to the weak shear case.

5. SUMMARY AND CONCLUSIONS

The beam heated, high triangularity, double–null NCS configuration has demonstrated enhanced confinement at high beta with robust and reliable operation. In general, NCS plasmas with enhanced confinement have a clear reduction in diffusive transport inside the region of negative shear. The reduced transport lowers the ion conductivity to the neoclassical level; the electron transport in comparison remains relatively unchanged. NCS discharges with an H–mode edge also have reduced ion transport in the outer region of the discharge resulting in neoclassical ion transport over the entire plasma cross–section. Larger values of negative shear further reduce the ion diffusivity in the L–mode edge discharges but not in the H–mode edge case. A reduction in particle transport also accompanies the reduction in energy transport in the NCS plasmas with an L–mode edge. Accompanying the reduced core transport in NCS discharges is the reduction in core fluctuations which is consistent with the suppression of η_i driven transport. Sheared $\mathbf{E}\times\mathbf{B}$ flow appears to play a key role in turbulence suppression. Future work will focus on understanding sources for anomalous core electron transport in the NCS regime as well as ion transport mechansims with low magnetic shear and an L–mode edge.

ACKNOWLEDGMENTS

This work was supported by the U.S. Department of Energy under Contract Nos. DE-AC03-89ER51114, DE-AC05-96OR22464, and DE-AC04-94AL85000 and Grant Nos. DE-FG03-86ER53266 and DE-FG03-95ER54294.

REFERENCES

[1] STRAIT, E.J., et al., Phys. Rev. Lett. **75** 4421 (1995).
[2] LAO, L.L., et al., Phys. Plasmas **3** 1951 (1996).
[3] RICE, B.W., et al., Phys. Plasmas **3** 1983 (1996).
[4] RICE, B.W., et al., Plasma Phys. Controlled Fusion **38** 869 (1996).
[5] LAZARUS, E.A., et al., Phys. Rev. Lett. **77** 2714 (1996).
[6] for example see references in SCHISSEL, D.P., et al., Nucl. Fusion **29** 185 (1989).
[7] DOYLE, E.J., et al., paper F1–CN–64/A6–4, this conference.
[8] STALLARD, B., et al., "Transport in Negative Central Magnetic Shear L–mode Plasmas in DIII–D," submitted to Nucl. Fusion.
[9] HAHM, T.S., BURRELL, K.H., Phys. Plasmas **2** 1648 (1995).
[10] WALTZ, R.E., et al., Phys. Plasmas **1** 2229 (1994).
[11] HINTON, F.L., STAEBLER, G.M., Phys. Fluids **B5** 1281 (1993).
[12] KOTCHENREUTHER, M., Bull. Am. Phys. Soc. **37** (1992) 1432.
[13] GREENFIELD, C.M., et al., "Transport in High Performance Weak and Negative Magnetic Shear Discharges in DIII–D," in Proc. 23rd Euro. Conf. on Contr. Fusion and Plasma Physics, Kiev, Ukraine, to be published.
[14] STAEBLER, G.M., HINTON, F.L., et al., Phys. Plasmas **1** 909 (1994).